Indonesian Journal of Material Research
***e*-ISSN: 2987-1654**
Vol. 5, No. 1, March 2027

Indonesian Journal of MATERIAL RESEARCH

Research Paper

Failure Mechanism Analysis of an AISI 52100 Condenser Fan Bearing in a Cold Storage Refrigeration System

Mustopa Kamal[1*], I Ketut Daging[1], Ade Hermawan[1], Samsi[1], Sobri[1]

[1]*Mechanical Engineering of Fisheries, Politeknik Ahli Usaha Perikanan, Jakarta, 12520, Indonesia*
[*]**Corresponding author**: mustopakamal1030@gmail.com

Abstract
Condenser fan bearings maintain stable airflow during heat rejection in cold storage refrigeration systems, where premature failure disrupts cooling reliability and increases maintenance demands. This case-specific study examines the failure characteristics of a single failed AISI 52100 bearing (FYH UCP309J/UC309) removed from a cold storage condenser fan after approximately six months of service, compared with a typical service life of 2–3 years. To evaluate whether material nonconformity or service-induced degradation contributed to the early failure, the investigation combined visual inspection with optical emission spectroscopy (OES), Vickers hardness testing at 5 kgf, and optical metallography at 1000× magnification on the sectioned outer ring. Visual inspection revealed raceway scoring, reduced grease availability, and brown discoloration. OES showed 0.981 wt.% C and 1.36 wt.% Cr with Fe as the balance, consistent with AISI 52100 steel. Hardness measurements yielded a mean of 709.5 HV, and metallography showed a martensitic matrix with spheroidal carbides and no evident pre-existing microstructural defects in the examined region. These material findings indicate conformity with expected bearing steel characteristics rather than bulk material failure, while raceway scoring, grease depletion, and discoloration point toward lubrication-related degradation as a plausible contributing mechanism. However, because no direct lubricant testing, operating telemetry, vibration analysis, or undamaged reference bearing were available, this interpretation remains strictly preliminary and non-exclusive.

Keywords
AISI 52100 Bearing Steel, Bearing Failure, Condenser Fan, Lubrication Degradation, Metallographic Analysis

Received: 19 September 2026, Accepted: 25 November 2026
https://doi.org/10.26554/ijmr.202751127

1. INTRODUCTION

Cold storage systems are essential components of the cold chain, as effective product preservation depends on the ability of refrigeration systems to maintain stable temperatures (Duarte et al., 2020; Svendsen et al., 2022). System reliability depends not only on thermal capacity but also on the performance of mechanical components involved in heat rejection, including the condenser and its fan drive assembly (Tanveer and Bradshaw, 2020). The condenser fan generates the airflow required for heat dissipation, while its bearings support the rotating shaft and maintain stable fan rotation with controlled friction (Tanveer and Bradshaw, 2020; Xu et al., 2023). Bearing failure can increase friction, vibration, and noise, potentially destabilizing fan rotation and disrupting refrigeration system operation (Tahmasbi et al., 2024; Xu et al., 2023). Premature bearing failure is therefore a significant concern because component service life can be influenced by complex interactions among material properties, lubrication conditions, loading, rotational speed, alignment, contamination, and operating conditions (Tahmasbi et al., 2024; Xu et al., 2023).

Previous studies have investigated bearing failures from various perspectives, including rolling contact fatigue, wear, lubricant degradation, contamination, vibration monitoring, and the effects of microstructure and hardness on material durability (Loaiza et al., 2023; Xu et al., 2023). In AISI 52100 bearing steel, chemical composition, hardness, martensitic structure, and carbide characteristics play important roles in wear resistance and material response to repeated contact loading (Li et al., 2024; Loaiza et al., 2023). However, these studies have often focused on tribological behavior, condition monitoring, or material characteristics individually, with many investigations conducted under controlled experimental conditions (Loaiza et al., 2023; Xu et al., 2023). In actual failure cases, surface scoring, discoloration, and reduced grease availability cannot independently establish a specific failure mechanism because these observations may be associated with multiple interacting factors (Jiang et al., 2025; Tahmasbi et al., 2024; Xu et al., 2023). To systematically discriminate among potential failure modes in the absence of continuous telemetry, specific evidence-based diagnostic criteria are established in this investigation: mechanical wear is evaluated through surface scoring, grooving, and material removal; rolling

contact fatigue (RCF) is characterized by surface or subsurface crack initiation, pitting, and spalling; and lubrication-related degradation is inferred from grease depletion, thermal discoloration, and localized adhesive smearing (Jiang et al., 2025; Popa et al., 2026; Tahmasbi et al., 2024).

This research gap is particularly relevant to the case of a condenser fan bearing operating in a large-capacity industrial cold storage refrigeration system that failed substantially earlier than its expected service life (approximately six months versus 2–3 years). Unlike prior failure analyses that predominantly examine high-speed turbomachinery, heavy industrial centrifugal fans (Jiang et al., 2025; Zhou et al., 2026), or laboratory-controlled tribological tests equipped with complete vibration and lubricant-monitoring datasets (Loaiza et al., 2023; Tahmasbi et al., 2024), field failures in commercial cold-storage condenser fan assemblies occur under continuous outdoor tropical humidity, thermal cycling, and intermittent manual maintenance where real-time condition monitoring is rarely installed. Consequently, maintenance engineers must frequently diagnose premature failures solely from retrieved hardware post-removal. This premature failure raises questions regarding whether the damage was primarily associated with material characteristics that deviated from the expected specification, material changes or degradation during service, or damage mechanisms arising from contact conditions and operational factors. Accordingly, this study addresses three research questions: (1) What are the characteristic visual features of the prematurely failed bearing? (2) Are the chemical composition, hardness, and microstructure consistent with the expected characteristics of AISI 52100 bearing steel? (3) Which failure mechanism is most consistent with the combined evidence obtained from the examinations?

This study aims to investigate the premature failure mechanism of an AISI 52100 condenser fan bearing in a cold storage refrigeration system using an integrated failure analysis approach. The investigation combines visual inspection to characterize the damage, chemical composition analysis using optical emission spectroscopy (OES), Vickers hardness testing, and metallographic examination to characterize the material microstructure. The specific novelty and contribution of this case study are threefold: first, it provides an empirical metallurgical and surface-damage benchmark for an in-service FYH UCP309J/UC309 pillow-block bearing operating in an under-reported cold-chain condenser fan application; second, it demonstrates an evidence-based differential diagnostic framework that evaluates whether base-metal chemistry, bulk hardness, or examined microstructural features show detectable deviations from AISI 52100 specifications within the scope of the retrieved outer-ring specimen; and third, it translates these constrained diagnostic findings into targeted, practical maintenance protocols for industrial cold-storage operators (Jiang et al., 2025; Ramadhan et al., 2023; Yudistirani et al., 2018; Zhou et al., 2026).

2. EXPERIMENTAL SECTION

2.1 Research Design and Materials

This study employed a descriptive-analytical case study approach to investigate the premature failure of a condenser fan bearing in a cold storage refrigeration system, following established failure analysis frameworks (Jiang et al., 2025; Xu et al., 2023). Specifically, the investigation was conducted on a single failed FYH UCP309J/UC309 pillow-block bearing unit–comprising a P309 cast-iron housing and a UC309 through-hardened AISI 52100/SUJ2 insert ball bearing with a 45 mm bore diameter–removed from a rooftop belt-driven axial condenser fan drive assembly at a large-capacity industrial cold storage facility (PT Kiat Ananda Solusindo, Cileungsi, West Java, Indonesia; Figure 1). According to the facility's asset register and preventive maintenance (PM) benchmark records, comparable condenser fan bearing units operating on adjacent units under similar duty typically achieve a service life of 24–36 months (2–3 years). In contrast, the maintenance replacement logbook documented that the investigated bearing was prematurely removed after approximately six months of continuous 24/7 outdoor rooftop operation under humid tropical ambient conditions ($\sim$ 25–35 $^{\circ}$C), representing roughly 17–25% of its expected benchmark service life, following operator walk-down reports of audible abnormal running noise and elevated housing vibration prior to shutdown.

Lubrication in service was performed via manual lever-gun grease application; immediate on-site dismounting inspection revealed depleted cavity grease, thickened brownish-black grease residue near the contact seal lips, and brown discoloration along the outer-ring raceway track, although no grease samples were retained for laboratory physicochemical testing (such as FTIR, viscosity, or water content analysis). Furthermore, no undamaged reference bearing or new specimen from the same installation was available for comparative characterization, representing a deliberate case-study sampling limitation that restricts comparative inference between failed and serviceable components. Continuous automated telemetry–including exact cumulative running hours, shaft rotational speed (RPM) logs, dynamic radial and axial bearing load measurements, continuous housing temperature histories, and vibration frequency spectra–was also uninstrumented in the plant logbooks and is explicitly treated as an analytical boundary in this investigation.

Material characterization was conducted at an accredited external laboratory (Politeknik Manufaktur Bandung, Order No. UF-260097) on the sectioned outer ring using an ARL 3460 optical emission spectrometer (OES; Report No. 097/Sp. Lab. Mat./Ext. Polman/III/2026) for elemental chemical analysis, a ZHU 250CL hardness tester (Zwick Roell; Report No. 096/Hv.Lab. Mat./Ext./Polman/III/2026) for Vickers hardness testing, and an Olympus GX71 optical microscope (Report No. 097/Mef. Lab/Ext. Polman/III/2026) for metallographic examination of the AISI 52100 bearing steel microstructure (Li et al., 2024). Systematic disassembly and detailed metallurgical inspection of the inner ring, rolling elements (balls), cage, and contact seals were outside the scope of the submitted outer-ring specimen.

© 2027 The Authors.



Figure 1. Location of the Condenser Fan Bearing in the Cold Storage Refrigeration System

2.2 Inspection and Testing Procedures

2.2.1 Visual Inspection

Visual inspection was conducted as the initial stage of failure analysis to identify the physical condition of the bearing and characterize surface damage based on ISO 15243 (ISO, 2017; Popa et al., 2026) and SKF failure analysis guidelines (Popa et al., 2026; SKF, 2020). The bearing was examined directly after removal from the condenser fan assembly (Figure 2). Qualitative grease inspection was performed on-site immediately upon dismounting and prior to solvent cleaning or sectioning, evaluating visual grease volume depletion inside the cavity, color shifts, consistency changes (thickening, drying, or caking), and darkened/brownish-black grease residue near the seal lips. However, no retained grease samples were collected or stored for laboratory physicochemical testing (such as FTIR, base-oil viscosity, or moisture content analysis). The inspection focused on the outer ring surface, wear patterns such as scoring, brown discoloration associated with thermal exposure, and the condition of the grease (Xu et al., 2023).

2.2.2 Chemical Composition Analysis

Chemical composition analysis was performed to determine the principal elemental constituents of the bearing material and assess their consistency with the AISI 52100 bearing steel specification in ASTM A295 (Adishesha, 2002; Mano and Ohana, 2021). The analysis was conducted using an ARL 3460 optical emission spectrometer (OES), following ASTM E415 (Gurău et al., 2026; Toledo et al., 2022) and the laboratory's internal work instruction IK 8-5.4-3-04 (Edition A, Revision 3). Prior to sparking, the outer-ring specimen surface was ground/machined with abrasive paper (60–120 grit) to remove oxide layers, rust, oil, or decarburization and expose clean base metal. Measurements were acquired across three distinct spark spots (single discharge per spot to avoid arc-burn bias) on clean areas, and reported values represent the arithmetic mean of the three readings. The test was performed at an ambient temperature of 23 °C and a relative humidity (RH) of 48%.

2.2.3 Vickers Hardness Testing

Vickers hardness testing was conducted to determine the hardness of the outer ring material and evaluate the consistency of its measured hardness values. Measurements were performed using a ZHU 250CL hardness tester (Zwick Roell) under a test force of 5 kgf (5000 gf), in accordance with laboratory testing procedures aligned with ASTM E92 for macro-Vickers hardness testing (while noting that ASTM E384 primarily governs microindentation forces up to 1 kgf). The test was conducted at an ambient temperature of 23 °C and an RH of 60%. Four indentation points were measured on the prepared sectioned outer-ring surface (ground and polished to a clean metallic finish with standard dwell time), and the arithmetic mean, sample standard deviation, and coefficient of variation were calculated to evaluate hardness consistency across the examined sites (Ahmed et al., 2025; Loaiza et al., 2023).

2.2.4 Metallographic Examination

Metallographic examination was performed to characterize the microstructure of the bearing material after failure. Specimen preparation, including sectioning, mounting, grinding, and polishing, followed ASTM E3 (Mazzatura et al., 2026). The polished surface was etched with 3% Nital in accordance with ASTM E407 (Ahuir-Torres, 2023; Escobar, 2007). The microstructure was then examined using an Olympus GX71 optical microscope at 1000× magnification to characterize the martensitic matrix and spheroidal carbide distribution (Jasim et al., 2023; Park, 2018; Vander Voort, 2004).

2.3 Data Analysis

Data analysis was conducted using an integrated, evidence-based failure analysis approach, following the general framework presented in ASM Handbook, Volume 11 (Miller et al., 2021). The analysis integrated the findings from visual inspection, chemical composition analysis, hardness testing, and metallographic examination. Visual inspection results were used to identify surface damage patterns and characteristics based on the failure mode classification in ISO 15243 (ISO, 2017). The chemical composition data obtained by optical emission spectroscopy

© 2027 The Authors.

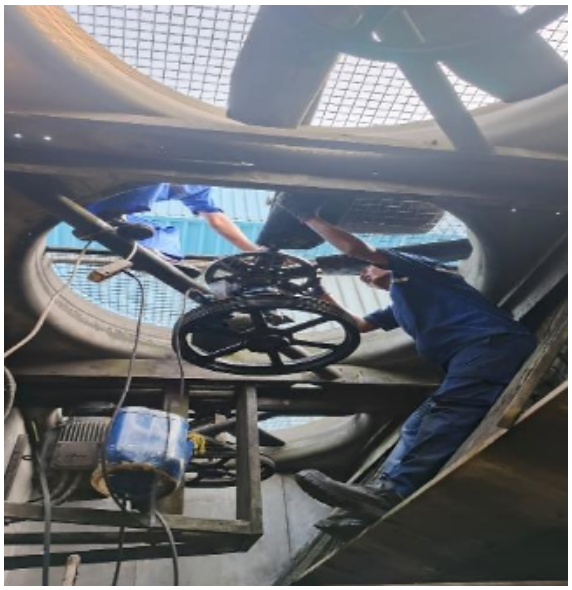


Figure 2. Fan Bearing Removal Process

(OES) were compared with the relevant material specification for AISI 52100 bearing steel. Hardness data were evaluated using the mean and variation of the measured values to assess the hardness level and consistency of the material. Metallographic findings were interpreted based on the observed phases and microstructural morphology (Mano and Ohana, 2021). Potential failure mechanisms—specifically tribological wear, rolling contact fatigue, and lubrication-related degradation—were evaluated systematically by cross-referencing surface morphology, material conformity, and service history against the established diagnostic criteria, while explicitly treating unmeasured field parameters as unverified contributing hypotheses rather than confirmed root causes (Jiang et al., 2025; Miller et al., 2021; Xu et al., 2023).

3. RESULTS AND DISCUSSION

3.1 Visual Inspection and Surface Damage Characteristics

Macroscopic visual inspection of the FYH UCP309J/UC309 condenser fan bearing, which failed prematurely after approximately six months of operation compared with the typical facility service life of 2–3 years, revealed distinct surface distress features and operational symptoms. The primary findings included external brown discoloration and grease depletion on the as-removed bearing assembly (Figure 3a), together with circumferential scoring and brownish surface discoloration along the concave raceway groove of the sectioned outer ring (Figure 3b), accompanied by progressive vibration and noise prior to shutdown. Mechanistically, the raceway scoring (Figure 3b) reflects localized mechanical distress caused by direct asperity-to-asperity contact. Under normal operating conditions, an elastohydrodynamic lubricating film separates the rolling elements from the raceways to prevent metal-to-metal interaction. A reduction in grease quantity or film integrity compromises this separation and accelerates surface wear. Because high-magnification stereomicroscopy or surface profilometry of the cleaned raceway was unavailable beyond the archived photographic records, scoring depth and fine wear-track morphology could not be quantified, and the visual evidence is interpreted qualitatively alongside the subsequent metallurgical tests. Nevertheless, the observed grease depletion is physically consistent with the onset of raceway scoring, aligning with Bhaumik and Paleu (2021), who demonstrated that lubricant-film degradation increases friction and wear-scar formation in AISI 52100 bearing steel.

Similarly, the brown-to-dark-brown surface discoloration observed across both the bearing exterior (Figure 3a) and the outer-ring raceway track (Figure 3b) does not uniquely signify bulk thermal overheating; rather, it may arise from three distinct or overlapping mechanisms: (i) localized frictional heating and mild surface oxidation caused by lubricant film breakdown and asperity contact; (ii) oxidative degradation and polymerization of mineral-oil-based grease into adherent brownish varnish or carbonaceous deposits under elevated operating temperatures; and (iii) tribo-chemical corrosion or fretting oxidation induced by moisture condensation and micro-slip at the housing–outer-ring interface in a humid tropical condenser environment. Because high-resolution macro-photography of the cleaned raceway, surface chemical analysis (e.g., EDS or FTIR of the surface film), and actual operating temperature histories were not obtained, these three mechanisms cannot be definitively separated. Therefore, the observed brown discoloration is interpreted conservatively as supportive evidence of localized frictional heating, lubricant oxidation deposits, or environmental surface oxidation rather than conclusive proof of severe thermal over-tempering.

Taken together, the reduced grease availability, raceway scoring, brown discoloration, and reported increases in noise and vibration indicate that lubrication-related degradation is the failure

© 2027 The Authors.



Figure 3. Macroscopic Visual Inspection of the Failed Bearing: (a) As-Removed FYH UCP309J/UC309 Assembly Exhibiting External Brown Discoloration and Depleted Cavity Grease (Yellow Oval and White Arrow); and (b) Sectioned Outer-Ring Concave Raceway Track Displaying Circumferential Scoring and Brownish Surface Discoloration

mechanism most consistent with the physical evidence. However, visual inspection alone cannot establish lubrication failure as the sole root cause. Furthermore, because the inner ring, rolling elements, and contact seals were not systematically inspected or documented after removal, potential contributing evidence from those components–such as seal lip wear or hardening permitting moisture and particulate ingress, localized spalling or smearing on the balls, or fretting and circumferential scoring on the inner ring–could not be evaluated. Consequently, the failure mode assignment relies primarily on outer-ring evidence, and primary or concurrent damage originating at the seals, rolling elements, or inner ring cannot be excluded. Other operational factors, including contamination, mounting conditions, shaft misalignment, abnormal belt or aerodynamic fan loading, and shaft fit condition, may also have contributed and are therefore evaluated alongside the chemical composition, hardness, and metallographic results in the following subsections.

3.2 Chemical Composition Analysis

The elemental composition of the sectioned outer ring (Figure 4) was determined by optical emission spectroscopy (OES) and compared against the standard specification for high-carbon chromium bearing steel (AISI 52100/SUJ2) defined in ASTM A295, as summarized in Table 1.

All principal alloying elements–specifically carbon (0.981 wt.%), chromium (1.360 wt.%), manganese (0.350 wt.%), and silicon (0.243 wt.%)–fall well within the prescribed ASTM A295 limits, while tramp impurity levels of phosphorus (0.009 wt.%) and sulfur (0.001 wt.%) remain well below the maximum threshold of 0.025 wt.%. In accordance with standard metallurgical practice, iron (measured at 96.898 wt.%) is designated as the compositional balance rather than an independent specification limit, ensuring that material conformity is evaluated strictly against the specified alloying and impurity thresholds.

Metallurgically, the verified carbon and chromium concentrations provide the necessary hardenability and carbide-forming capacity required for through-hardened bearing raceways to achieve high rolling-contact wear resistance. Consequently, within the sampled locations of the outer ring, the OES results show no evidence of bulk chemical nonconformity, off-grade steel substitution, or excessive tramp-element levels as primary contributors to the premature failure.

3.3 Vickers Hardness Testing

Macro-Vickers hardness measurements (5 kgf test load) were obtained at four locations across the transverse cross-sections of the sectioned outer ring–Points 1 and 2 on the left wall and Points 3 and 4 on the opposing right wall ($\sim 180^{\circ}$ apart) adjacent to the discolored raceway track (Figure 5)–yielding individual values of 712, 703, 713, and 710 HV5, respectively (Table 2). The measurements yielded an arithmetic mean hardness of 709.5 HV5 (approximately 60.5 HRC), with a low sample standard deviation of 4.51 HV5 and a coefficient of variation of 0.64%. For through-hardened AISI 52100/SUJ2 bearing rings quenched and low-temperature tempered in accordance with ASTM A295, standard specification hardness typically falls within 58–64 HRC ($\sim$ 653–800 HV) (Li et al., 2024; Loaiza et al., 2023; Yudistirani et al., 2018). The measured mean of 709.5 HV5 lies within this expected industrial range, indicating that the examined bulk cross-sectional substrate is consistent with standard through-hardened and tempered AISI 52100 material.

Furthermore, the close agreement between the opposing cross-sectional walls (703–712 HV5 on the left section versus 710–713 HV5 on the right section) indicates uniform bulk substrate hardness across the sampled regions, showing no evidence of widespread circumferential thermal softening at those locations. Nevertheless, because these four macro-Vickers indentations sampled only four discrete cross-sectional sites rather

© 2027 The Authors.



Figure 4. Specimen Used for Chemical Composition Analysis

Table 1. Chemical Composition of the Bearing Outer-Ring Material Compared with the Reference Specification for AISI 52100/SUJ2 Steel

Element	Measured Composition (wt.%)	Reference Composition (wt.%)
Carbon (C)	0.981	0.980-1.100
Chromium (Cr)	1.360	1.300-1.600
Manganese (Mn)	0.350	0.250-0.450
Silicon (Si)	0.243	0.150-0.350
Phosphorus (P)	0.009	$\leq$ 0.025
Sulfur (S)	0.001	$\leq$ 0.025
Iron (Fe)	96.898	Balance

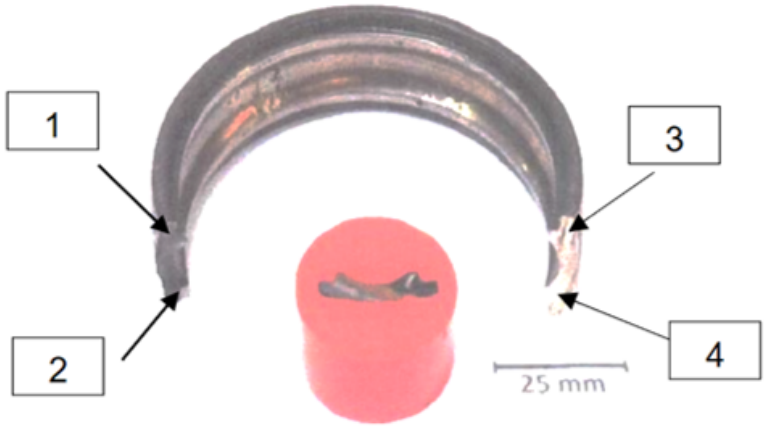


Figure 5. Sectioned Outer-Ring Specimen of the Failed FYH UCP309J/UC309 Bearing Illustrating the Four Macro-Vickers Indentation Locations on the Left (Points 1 and 2) and Opposing Right (Points 3 and 4) Transverse Cross-Sectional Walls

than a subsurface microhardness depth profile directly beneath the worn raceway track or the uninspected bearing components, localized near-surface softening or localized heat-treatment variations elsewhere in the bearing assembly cannot be excluded.

3.4 Metallographic Examination and Failure Mechanism Evaluation

Transverse cross-sectional optical metallography of the failed outer ring (Figure 6) revealed a homogeneous, dark-etched tem-

© 2027 The Authors.

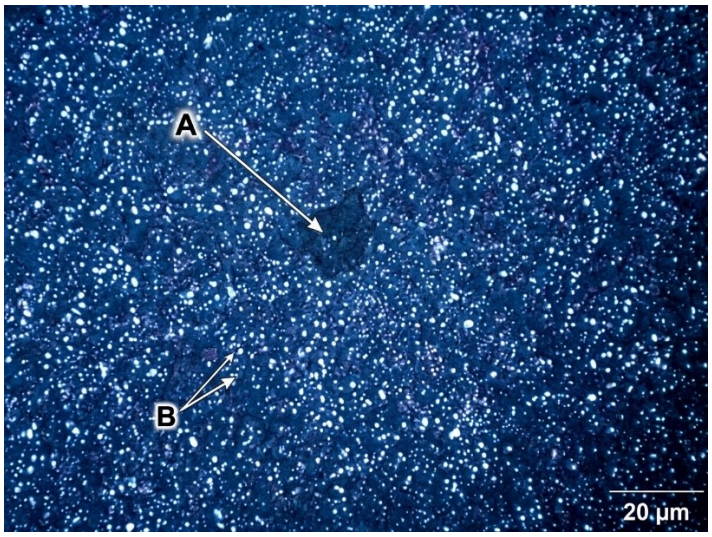


Figure 6. Optical Micrograph of the Transverse Cross-Section of the Failed AISI 52100 Bearing Outer Ring (3% Nital Etch, 1000× Magnification), Showing (A) the Dark-Etched Tempered Martensitic Matrix and (B) Uniformly Dispersed Fine Spheroidal Carbides

Table 2. Macro Vickers Hardness (HV5) Test Results

Measurement Point	d_1 (μm)	d_2 (μm)	d_{avg} (μm)	HV
1	114.1	114.1	114.1	712
2	114.9	114.8	114.9	703
3	114.4	113.7	114.1	713
4	114.5	114.1	114.3	710
Average HV				709.5
Standard Deviation (SD)				4.51
Coefficient of Variation (CV)				0.64%

Note: HV5 denotes Vickers hardness measured under a 5 kgf (49.03 N) load in accordance with ASTM E92.

pered martensitic matrix (A) containing uniformly dispersed, fine spheroidal carbide particles (B). Within the examined field, no carbide banding, continuous grain-boundary carbide networks, surface decarburization, coarse non-metallic inclusions, or quench-induced microcracks were observed. Because quantitative image analysis and calibrated particle-size measurements were not performed on the single archived optical micrograph due to resolution constraints, the carbide dispersion is evaluated qualitatively rather than by numerical size distribution.

Within the single examined optical field, these microstructural features are consistent with the OES chemical composition and 709.5 HV5 macrohardness results, showing no evident manufacturing-related microstructural anomalies or bulk thermal over-tempering in the sampled region. However, because metallographic observation was limited to a single archived transverse field of the outer ring, localized microstructural defects, inclusion clusters, or heat-treatment non-uniformities in unexamined regions or in the inner ring and rolling elements cannot be entirely ruled out. Evaluating competing failure hypotheses against the integrated evidence indicates that lubrication-related degradation leading to tribological wear (raceway scoring) is the most plausible mechanism consistent with the observed grease depletion, surface scoring, and brown discoloration alongside intact bulk steel properties. Conversely, classical subsurface rolling contact fatigue (RCF) is less directly supported given the absence of macroscopic raceway spalling—although single-field optical microscopy cannot exclude localized microscopic subsurface fatigue damage immediately beneath the worn contact track—while particulate or moisture ingress and installation misalignment remain plausible, unverified contributing factors in the absence of lubricant physicochemical testing, vibration spectra, and operational load or temperature logs (Jiang et al., 2025; Miller et al., 2021; Xu et al., 2023).

4. CONCLUSIONS

This study concludes that, within the limits of the examined outer-ring specimen, no bulk chemical nonconformity, abnormal macrohardness, or apparent microstructural defects were detected to explain the premature failure of the investigated FYH UCP309J/UC309 condenser fan bearing after approximately six months of operation. OES analysis (0.981 wt.% C, 1.36 wt.% Cr, Fe balance), Vickers hardness testing (mean hardness of 709.5 HV), and optical metallography (tempered martensitic matrix with dispersed spheroidal carbides) confirmed that the bearing mate-

© 2027 The Authors.

rial conformed to AISI 52100/SUJ2 steel specifications. Based on the integrated physical and metallurgical evidence, lubrication-related degradation during service represents the most plausible mechanism consistent with the observed raceway scoring, grease depletion, and brown surface discoloration-distinct from an experimentally confirmed root cause, as direct lubricant testing, operating temperature logs, vibration spectra, and inspection of the inner ring, rolling elements, and seals were not conducted.

Consequently, concurrent contributing factors-including mo isture or particulate ingress, shaft misalignment, abnormal belt or aerodynamic fan loading, and seal lip wear-remain unverified hypotheses requiring direct field instrumentation. To prevent premature bearing recurrence in industrial cold-storage condenser fan assemblies, preventive maintenance should implement four case-specific practical checks: (1) lubrication management, by verifying grease suitability for humid outdoor tropical duty, enforcing operating-hour-based relubrication intervals, and inspecting purged grease for darkening or water emulsification; (2) sealing and housing integrity, by inspecting contact lip seals and pillow-block covers for hardening, wear, or ingress gaps; (3) alignment and mounting verification, by checking shaft coaxiality, set-screw torque, belt tension, and fan-blade balance during commissioning; and (4) operating-history tracking, by logging cumulative running hours, housing skin temperatures via infrared thermography, and baseline vibration levels for early distress detection.

5. ACKNOWLEDGEMENT

The authors would like to thank PT KIAT ANANDA SOLUSINDO for granting permission and providing data support for this research conducted at the cold storage facility in Pangkalan 12, Cileungsi, West Java, Indonesia.

REFERENCES

Adishesha, P. K. (2002). Effect of Steel Making and Processing Parameters on Carbide Banding in Commercially Produced ASTM A-295 52100 Bearing Steel. *ASTM Special Technical Publication*, (1419); 27–46

Ahmed, F. L., S. S. Abdullah, S. K. Jasim, and A. H. Ghazi (2025). Study the Effect of DBD Plasma on the Mechanical Properties of Polymer. *Indonesian Journal of Material Research*, (3(2)); 41–46

Ahuir-Torres, J. I. (2023). Microscopy Techniques to Analyse the Characteristics of the Metallic Materials. *Journal of Materials and Electronic Devices*, (1(1)); 33–53

Bhaumik, S. and V. Paleu (2021). Wear and Rolling Contact Fatigue Analysis of AISI 52100 Bearing Steel in Presence of Additivated Lubricants. *MDPI*, (11(6)); 1–17

Duarte, A. M., F. Silva, F. R. Pinto, S. Barroso, and M. M. Gil (2020). Quality Assessment of Chilled and Frozen Fish — Mini Review. *Foods*, (25(9)); 1–26

Escobar, J. R. E. (2007). *Microetching Metals and Alloys 1 ASTM E407*. Soluciones Utilizadas Para Decapado de Metales y Aleaciones

Gurău, L., F. Marin, M. Marin, C. Ştefănescu, and G. Gurău (2026). Failure Case Study Series Part Two: Failure Analysis of Roller Guides in a Wire Rod Rolling Mill. *Annals of the University Dunarea de Jos of Galati: Fascicle IX, Metallurgy & Materials Science*, (49(2)); 29

ISO (2017). *Rolling Bearings — Damage and Failures — Terms, Characteristics and Causes*. 15243. International Organization for Standardization

Jasim, S. A., A. A. Habeeb, and A. Kadhim (2023). The PLD Method Enhances the Surface Properties of 316 and 304 Stainless Steel by Coating ZnO Films. *Indonesian Journal of Material Research*, (1(3)); 91–98

Jiang, T.-H., S. Zhou, A.-X. Pan, Y.-H. Che, G.-Q. Li, H.-J. Xu, Y. Gong, and Z.-G. Yang (2025). Failure Analysis of the Abnormal Wear of Rolling Bearing in the Centrifugal Fan for Nuclear Power Plant. *Engineering Failure Analysis*, (171); 109353

Li, Y., Z. Jiang, L. Li, P. Wang, D. Li, and W. Xue (2024). Wear Behavior and Damage Characterization for AISI 52100 Bearing Steels: Effect of Hardness and Spherical Carbides. *Journal of Materials Research and Technology*, (30(April)); 8359–8370

Loaiza, T., R. P. Babu, S. Ooi, and P. Hedström (2023). Refining the Mechanistic Understanding of Microstructural Decay During Rolling Contact Fatigue in 52100 Bearing Steel Tempered at High Temperature. *Journal of Materials Science*, (58(44)); 17093–17112

Mano, H. and T. Ohana (2021). Evaluation of Anti-Adhesion Characteristics of Diamond-Like Carbon Film by Combining Friction and Wear Test with Step Loading and Weibull Analysis. *Materials*, (14(2746)); 1–13

Mazzatura, I., G. Macoretta, F. Mattei, S. Caprili, and R. Valentini (2026). Implementation of a Simplified Code for Determining the Grain Dimension in Simple Metallographic Structures. *Metallography, Microstructure, and Analysis*; 1–18

Miller, B. A., R. J. Shipley, R. J. Parrington, and D. P. Dennies (2021). Failure Analysis and Prevention. In *ASM Handbook*, 11. ASM International, Materials Park, OH, page 2583

Park, O. H. (2018). LIFT—Additive Manufacturing for Lightweighting. ASM World Headquarters, Materials Park, OH

Popa, C., C. Sorin, G. G. Ojoc, M. Constandache, V. Azamfirei, and L. Deleanu (2026). Damage Classification and Terminology for Machine Components: A Review of Standardization and Diagnostic Practice. *Machines*, (14(448)); 1–46

Ramadhan, F., Z. Fuadi, R. Kurniawan, D. Rahmadiawan, and A. R. Nasution (2023). Pengaruh Penambahan Nano-Aditif Ke Dalam Fluida Polyolester Terhadap Gesekan Dan Keausan Material AISI52100 Vs Cast Iron. *Jurnal Rekayasa Material, Manufaktur Dan Energi*, (6(1)); 54–65

SKF (2020). Bearing Damage and Failure Analysis Handbook. *SKF Publication*, (21)

Svendsen, E. S., K. N. Widell, G. M. Tveit, T. S. Nordtvedt, S. Uglem, I. Standal, and K. Greiff (2022). Industrial Methods of Freezing, Thawing and Subsequent Chilled Storage of Whitefish. *Journal of Food Engineering*, (315(110803)); 1–13

Tahmasbi, D., H. Shirali, S. Sajad Mousavi Nejad Souq, and M. Es-

© 2027 The Authors.

lampanah (2024). Diagnosis and Root Cause Analysis of Bearing Failure Using Vibration Analysis Techniques. *Engineering Failure Analysis*, (158); 107954

Tanveer, M. M. and C. R. Bradshaw (2020). Quantitative and Qualitative Evaluation of Various Positive-Displacement Compressor Modeling Platforms. *International Journal of Refrigeration*, (119); 48–63

Toledo, H., J. Martínez-Gómez, and J. F. Nicolalde (2022). Selection of Rear Axle Tip Alternative Material of a Car by Multi-Criteria Means. *International Journal of Mathematics in Operational Research*, (21(1)); 46–66

Vander Voort, G. F. (2004). Metallography and Microstructures. In *ASM Handbook*, 9. ASM International, pages 493–512

Xu, F., N. Ding, N. Li, L. Liu, N. Hou, N. Xu, W. Guo, L. Tian, H. Xu, C.-M. Lawrence Wu, X. Wu, and X. Chen (2023). A Review of Bearing Failure Modes, Mechanisms and Causes. *Engineering Failure Analysis*, (152); 107518

Yudistirani, S. A., K. H. Mahmud, and E. Diniardi (2018). Analisis Kekerasan Pada Outer Ring dan Inner Ring Hasil Proses Heat Treatment. *Jurnal Teknologi*, (10(1)); 83–88

Zhou, S., A.-X. Pan, T.-H. Jiang, Y. Gong, and Z.-G. Yang (2026). Failure Analysis and Mechanism Study of Abnormal Wear in Nuclear Power Plant Fan Bearing. *Engineering Failure Analysis*, (189); 110694

© 2027 The Authors.